



Research paper

Novel pyridinedicarboxamide derivatives and a polymeric copper(II) complex: Synthesis, structural characterization, electrochemical behavior, catalytic and cytotoxic studies



Sara Abdolmaleki, Mohammad Ghadermazi*

Department of Chemistry, Faculty of Science, University of Kurdistan, Sanandaj, Iran

ARTICLE INFO

Article history:

Received 10 August 2016

Received in revised form 16 February 2017

Accepted 19 February 2017

Available online 27 February 2017

Keywords:

Amide-based ligands

One-dimensional polymeric complex

Electrochemical behavior

Catalytic activity

Cytotoxicity

ABSTRACT

Two new amide-based ligands, *N,N'*-bis(2-carboxylphenyl)-2,6-pyridinedicarboxamide (**L1**), *N,N'*-bis(2-carboxyphenyl ethyl ester)-2,6-pyridinedicarboxamide (**L2**) and a one-dimensional polymeric complex from reaction between (**L1**) and $\text{Cu}(\text{NO}_3)_2 \cdot 3\text{H}_2\text{O}$ with the formula of $\{[\text{Cu}(\text{CPCP})(\text{DMAP}) \cdot 3\text{H}_2\text{O}]_n\}$ [where DMAP is 4-dimethylaminopyridine and CPCP is 6-(2-carboxylatophenylcarbamoyl) picolinate] were synthesized. These compounds have been characterized spectroscopically and their molecular structures were determined by single-crystal X-ray diffraction. Also, thermal analysis (TGA/DTA) was carried out on complex (**3**). Possible mechanisms were proposed for esterification and hydrolysis of (**L1**). Study of electrochemical behavior of compounds using cyclic voltammetry at E of -1.0 to $+1.0$ V showed two redox couple for complex (**3**) corresponding to $\text{Cu}(\text{I})/\text{Cu}(\text{0})$ and $\text{Cu}(\text{II})/\text{Cu}(\text{I})$ at E^0 of -0.26 to 0.08 V versus Ag/AgCl . Ligands (**L1**) and (**L2**) did not exhibit any wave in the investigated potential range. Also, complex (**3**) was evaluated for catalytic activity on the oxidation of aromatic and aliphatic alcohols by changing parameters such as the amount of catalyst, oxidant and also reaction temperature. The outstanding catalytic performance of complex (**3**) was confirmed by selective conversion of alcohols to the corresponding aldehydes. The cytotoxic effect of compounds was evaluated using oxaliplatin as a positive control against MCF7 (a human breast cancer), HT29 (a human colon adenocarcinoma) and βTC (a mouse beta pancreatic) cell lines. The cancerous cells exhibited the highest sensitivity to compound (**3**) with IC_{50} values about $1\text{--}10$ μM .

© 2017 Elsevier B.V. All rights reserved.

1. Introduction

For a long time coordination chemistry of organic amides have been attracted much attention of inorganic chemists as an important part of current chemical problems [1–3]. Molecules containing the amide functionality are a class of compounds with variety of applications in different fields of chemistry and biochemistry. The favorable chemical properties which led to more accurate study of these compounds include variable bonding modes for complexation of metal ions [4], stabilization of metal ions in their different oxidation states [5] and selective extraction of metal ions. From the point of biochemistry, amidic linkages are investigated as the main building units in natural macromolecules such as proteins and polypeptides [6] and synthetic macromolecules such as nylons and Kevlar® [7]. The versatile coordination behavior and potential hemilability of hybrid ligands containing (N, O) made

them to be investigated for the synthesis of supramolecular structures [8]. The steric environment and electronic properties of amidic ligands are affected by changing acyl groups or substituents on the nitrogen atom. Many amidic complexes of transition metals and rare-earth metals were studied due to their high activities in catalytic transformations, ring-opening polymerization of lactones, oligomerization and polymerization of ethylene and insertion reactions [9]. Formation of metal complexes with acidic organic ligands, in which the acid group is usually a hydroxide, an amide NH, or a thiol, is facilitated via the deprotonation of the ligand by the addition of a base such as triethylamine, sodium hydride, or use of the corresponding metal acetate [10]. The high donor ability of tertiary amides such as DMA and DMF (which are usually used as solvent) makes it possible for them to coordinate with metal ions in many complexes, directly [11]. On the other hand, metal ions with capability of substituting for amidic hydrogen can coordinate strongly to the amide group [12]. The molecular geometries are affected by the bulky amide groups in these structures [13].

* Corresponding author.

E-mail address: mghadermazi@yahoo.com (M. Ghadermazi).

Multidentate heterocyclic ligands of pyridylcarboxamides have an important position in biochemistry and coordination chemistry. Several researches have been carried out on bonding and structural motifs involving at this class of ligand; from isolated macrocycles and helicates to dynamic porous frameworks [14]. The regular hydrogen bonding of the amide groups can be used for a special design contributing to the robustness of the frameworks and their thermal stability [15]. A large number of high-valence copper complexes with amide-based ligands were investigated as biomimetic models and catalytic oxidants. The study of coordination structures of $\text{Cu}^{2+/3+}$ complexes containing amidic ligands demonstrated that N_{amide} donors are effective in bringing out and stabilizing the high oxidation state of a metal ion [16].

Many transition metal complexes possess capability of enhancing cellular radiation damage both *in vitro* and *in vivo*. Copper(II) ion was studied to modify the radiation response in both mammalian and bacterial cells. The radiosensitizing mechanism in mammalian cells suggested the involvement in reduction of copper(II) to copper(I). Recently, it was recognized that the radiosensitization process may be related to the radiation induced DNA damage, biological damage sensitized by copper ions involve nucleobases and different structure of copper complexes which might bind with double-helical DNA and promote double-strand DNA damage [17]. Although many transition metal complexes have been synthesized and their applications were investigated in various fields [18–20], the biological relevance and rich catalytic activity of copper complexes containing amidic nitrogen donors encouraged us to prepare such compounds. For example copper (II) complexes in addition to their effects on cancer treatment [21–23], can be effective as catalysts for the oxidative organic transformations involving the oxidation of alcohols, alkanes, alkenes and thioethers [24].

These results, along with our interest to design new compounds with catalytic and cytotoxic activity, led us to synthesize and study of new amidic ligands from the reaction of pyridine-2,6-dicarboxylic acid and 2-aminobenzoic acid and also, a Cu(II) complex from (**L1**) [25]. It is noteworthy that despite high stability of amide groups [26], X-ray studies exhibited that one of the amidic bonds was hydrolyzed during the complexation of ligand (**L1**) [27] and an unsymmetrically polymeric Cu(II) complex was synthesized. In this paper, possible mechanisms and some effective factors on the hydrolysis of amides are discussed.

2. Experimental

2.1. Materials and apparatus

Pyridine-2,6-dicarboxylic acid, 2-aminobenzoic acid, 4-dimethylaminopyridine (DMAP), thionyl chloride, hexanol, benzyl alcohol and its derivatives were purchased from the commercial sources and used as received. The solvents were distilled for all synthetic works. Melting points were obtained on an Electrothermal IA-9100 apparatus. The FT-IR spectra were recorded on a Bruker Vector 22 FT-IR spectrometer using KBr pellets. Electronic spectra were recorded on Specord 210, Analytik Jena spectrophotometer in the range of 200–900 nm at room temperature. Microanalyses (C, H, N) were measured with a Perkin-Elmer 2004(II) elemental analyzer. The ^1H NMR spectra (400 MHz) were obtained from Bruker Ultrashield 400 spectrometer. Thermal behavior was measured with a PL-1500 TGA apparatus with heating rate of 10 °C/min in N_2 atmosphere. The mass spectroscopy (MS) was determined using an Agilent (USA) spectrophotometer. Electrochemical experiments were performed using a $\mu\text{AUTOLAB}$ modular electrochemical system (ECO Chemie, Utrecht, the Netherlands) equipped with a PGSTAT type III module driven by GPES software in conjunction with a conventional three-electrode system an Ag/

AgCl/3 M KCl and platinum wire as reference and counter electrode respectively and a GC as working electrode. The working electrode was polished with aluminum oxide powder on chamois leather and the electrolyte was deoxygenated with nitrogen gas prior to the analysis.

2.2. Synthesis procedures

2.2.1. Synthesis of *N,N'*-bis(2-carboxylphenyl)-2,6-pyridine-dicarboxamide (**L1**)

Synthetic route of compounds are displayed in Scheme 1. At first, anhydrous thionyl chloride (25 mL) was added to pyridine-2,6-dicarboxylic acid (1 mmol, 0.167 g) and refluxed at 80–90 °C under argon atmosphere for 3 h until a clear yellow solution was obtained. The excess thionyl chloride was removed under reduced pressure. The product was dried in vacuum, cooled and obtained white precipitate was dissolved in dichloromethane (15 mL) and then, 2-aminobenzoic acid (2 mmol, 0.274 g) in dry pyridine (20 mL) was added to it. The color of the solution is changed slowly from dark green to brown, with occasional stirring. The solution was stirred overnight at room temperature and during the time period light yellow precipitate was formed. The precipitate was filtered off, washed with water, dried in the air and recrystallized from methanol. Yield (89%). M.p: 279 °C. Found (calc. for $\text{C}_{21}\text{H}_{15}\text{N}_3\text{O}_6$): C 62.11 (62.23), H 3.55 (3.70), N 10.49 (10.37)%. Selected IR bands (KBr pellet, cm^{-1}): 3446 m (ν_{NH}), 1693 s, 1660 s (ν_{CO}), UV-Vis: λ_{max} (CH_3OH , nm), 235. EI MS: m/z 405, M^+ .

2.2.2. Synthesis of *N,N'*-bis(2-carboxyphenyl ethyl ester)-2,6-pyridine-dicarboxamide (**L2**) compound (**L1**) (0.5 mmol, 0.203 g) was dissolved in ethanol (30 mL) and sulfuric acid was added to it (100 μL)

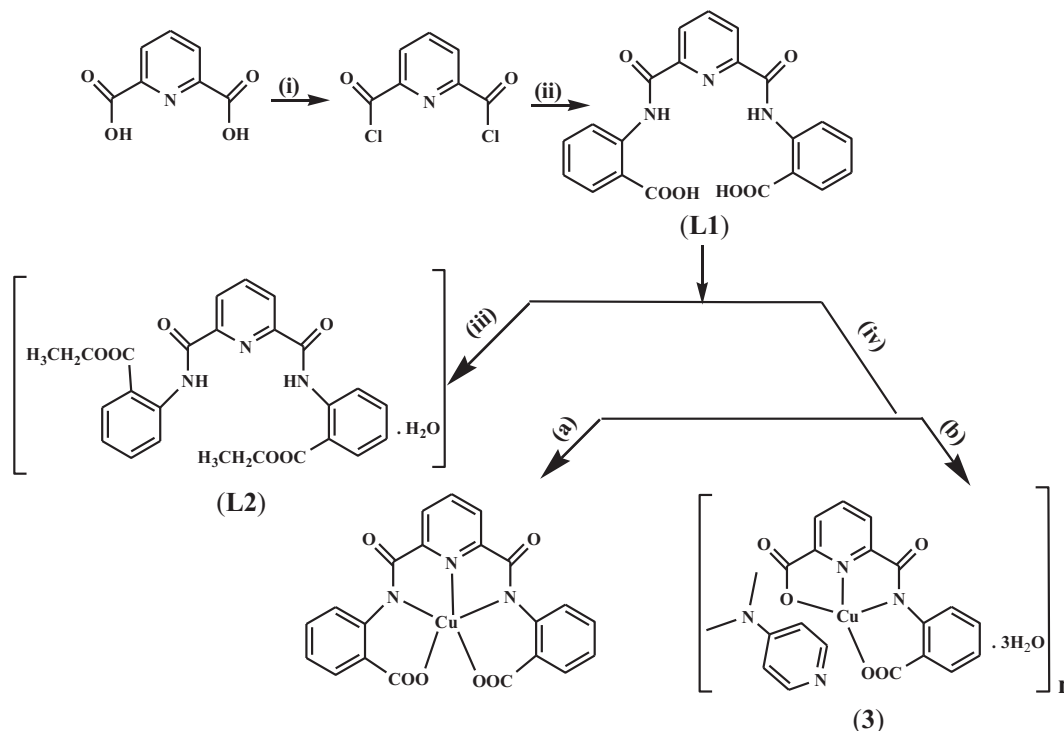
The solution was stirred 10 min at room temperature. The cubic yellow single crystals were formed after 15 days. Yield (70%). M.p: 287 °C. Found (calc. for $\text{C}_{25}\text{H}_{25}\text{N}_3\text{O}_7$): C 62.81 (62.63), H 5.43 (5.21), N 8.64 (8.76)%. Selected IR bands (KBr pellet, cm^{-1}): 3351 m (ν_{NH}), 1733 s, 1660 s (ν_{CO}), UV-Vis: λ_{max} (CH_3OH , nm), 227. EI MS: m/z 479, M^+ .

2.2.3. Synthesis of $\{[\text{Cu}(\text{CPCP})(\text{DMAP})\cdot 3\text{H}_2\text{O}]\}_n$ (**3**)

Under aerobic conditions, aqueous solution of DMAP (0.48 mmol, 0.058 g) was added to a stirring aqueous solution of ligand (**L1**) (0.12 mmol, 0.048 g). The obtained suspension was stirred at 70 °C for 2 h until a light yellow solution was produced. Then aqueous solution of $\text{Cu}(\text{NO}_3)_2\cdot 3\text{H}_2\text{O}$ (0.12 mmol, 0.028 g) was added and the mixture was refluxed at 100 °C for 2 h and evaporated to dryness. The crude product was recrystallized from distilled water as green needle-like crystals. Yield (71%). M.p: 289 °C. Found (calc. for $\text{C}_{21}\text{H}_{23}\text{N}_4\text{O}_8\text{Cu}$): C 48.15 (48.27), H 4.31 (4.40), N 10.69 (10.72)%. Selected IR bands (KBr pellet, cm^{-1}): 1647 s, 1604 s (ν_{CO}), UV-Vis: λ_{max} (CH_3OH , nm), 231. EI MS: m/z 522, M^+ .

2.3. X-ray crystallography

The X-ray measurement of single crystal of compounds (**L1**), (**L2**) and (**3**) were carried out using a Bruker SMART APEX II diffractometer equipped with a CCD area detector at 298 K, with graphite-monochromated Mo-K α radiation, $\lambda = 0.71073 \text{ \AA}$. All refinements were done by the full-matrix least-squares method on F^2 using the SHELX-97 program and absorption corrections were performed using the SADABS program [28a–e]. Software including Bruker APEX II (data collection and cell refinement) and WinGX (publication material) were properly employed [29]. The molecular graphic programs including DIAMOND [30] and MERCURY were used [31]. The crystal and structural refinement data for compounds are given in Table 1.



Scheme 1. Synthesis route of ligands and polymeric Cu(II) complex. i: SOCl_2 , ii: 2-aminobenzoic acid in dry pyridine, iii: recrystallized in ethanol, iv: $\text{Cu}(\text{NO}_3)_2 \cdot 3\text{H}_2\text{O}/\text{DMAP}$. (a) Predicted complex, (b) Formed complex of $\{[\text{Cu}(\text{CPCP})](\text{DMAP}) \cdot 3\text{H}_2\text{O}\}_n$.

Table 1
Crystallographic and structural refinement data for compounds (L1), (L2) and (3).

	(L1)	(L2)	(3)
Formula	$\text{C}_{21}\text{H}_{15}\text{N}_3\text{O}_6$	$\text{C}_{25}\text{H}_{25}\text{N}_3\text{O}_7$	$\text{C}_{21}\text{H}_{23}\text{N}_4\text{O}_8\text{Cu}$
Formula weight	405.36	479.48	522.96
Temperature (K)	298 (2)	298 (2)	298(2)
Wavelength λ (Å)	0.71069	0.71073	0.71073
Crystal system	Orthorhombic	Monoclinic	Monoclinic
Space group	<i>Pbca</i>	<i>P2₁/n</i>	<i>P2₁/n</i>
a (Å)	18.491(4)	10.286(2)	15.636(3)
b (Å)	7.5742(15)	7.2038(14)	6.9522(14)
c (Å)	26.016(5)	30.590(6)	20.971(4)
α (°)	90.00	90.00	90
β (°)	90.00(3)	94.80(3)	100.44(3)
γ (°)	90.00	90.00	90
Volume (Å ³)	3643.7(13)	2258.7(8)	2242.0(8)
Z	8	4	4
Density (calc.) (g cm ⁻³)	1.478	1.410	1.549
θ ranges for data collection (°)	2.70–25.00	2.67–25.00	2.65–25.00
<i>F</i> (000)	1680	1008	1080
Absorption coefficient (mm ⁻¹)	0.111	0.104	1.030
Index ranges	$-21 \leq h \leq 20, -9 \leq k \leq 9, -30 \leq l \leq 30$	$-11 \leq h \leq 12, -8 \leq k \leq 8, -36 \leq l \leq 36$	$-18 \leq h \leq 18, -8 \leq k \leq 8, 0 \leq l \leq 24$
Reflections collected/unique	20,731/3196 [<i>R</i> (int) = 0.1133]	12,079/3943 [<i>R</i> (int) = 0.0419]	7347/3949 [<i>R</i> (int) = 0.0695]
Data/restraints/parameters	3196/0/288	3943/1/326	3949/0/312
Final <i>R</i> indices [<i>I</i> > 2σ(<i>I</i>)] <i>R</i> ₁ , <i>wR</i> ₂	0.0391, 0.0668	0.0515, 0.1328	0.0558, 0.1416
<i>R</i> indices (all data) <i>R</i> ₁ , <i>wR</i> ₂	0.1288, 0.0827	0.0854, 0.1418	0.1149, 0.1498
Goodness of fit on <i>F</i> ² (<i>S</i>)	1.009	0.922	0.921
Largest diff peak and Hole (e Å ⁻³)	0.161, -0.183	0.210, -0.447	0.431, -0.334

2.4. Typical procedure for the study of catalytic properties

To investigate the catalytic activity of complex (3), oxidation of primary alcohols into the corresponding carbonyl compounds was carried out [32]. Benzyl alcohol was selected as a model substrate for oxidation process. As an initial test, different amounts of complex from 0.01 to 0.05 g in acetonitrile solvent were mixed with

30 μL of hydrogen peroxide (30%) as an oxidant and benzyl alcohol (0.5 mmol, 0.05 g) was added to the mixture at room temperature. Also, the reaction was run in the absence of catalyst. Then, by changing of parameters such as the amount of oxidant from 30 to 65 μL and temperature from 20 to 70 °C, optimized conditions for oxidation of benzyl alcohol to benzaldehyde was evaluated. After finding the optimized conditions for benzyl alcohol, oxidation

of its derivatives and hexanol (0.5 mmol substrate) were studied in the same way. The reaction progress was monitored by TLC in a regular alternative time. After completion of the reactions and removing of the solvent, the homogeneous catalyst was separated from the reaction mixture by addition of water (5.0 mL). Then, the organic phase was separated by addition of chloroform (10.0 mL) and dried over Na_2SO_4 . The product was purified by chromatography on silica gel (ratio of eluent: hexane/ethyl acetate from 1:10 to 1:5). Yields were obtained by weighting of isolated products. All products were known by MS and ^1H NMR spectroscopy [9,24].

2.5. Cell culture and cytotoxicity assays

MCF7 (a human breast cancer), HT29 (a human colon adenocarcinoma) and βTC (a mouse beta pancreatic) cell lines were provided from the Pasteur Institute (Iran), in this study. Cells were grown in 25 cm^2 culture flasks using DMEM (Gibco, Germany) supplemented by 10% (v/v) FBS (fetal bovine serum) and penicillin/streptomycin (100 U/mL, 100 mg/mL) at 37 °C in a humidified atmosphere of 5% CO_2 . They were sub-cultured regularly using of trypsin–ethylenediamine tetra acetic acid (EDTA-PBS) solution (Ben Yakhte, Iran). MCF7, HT29 and βTC cells were incubated into 96-well tissue culture plates at a density of 5×10^4 cells/well in 200 μL of complete media at 37 °C and below 5% CO_2 in a humidified incubator allowing the cell adhesion for 24 h. Stock solutions of (**L1**), (**L2**) and (**3**) were prepared in DMSO (below 0.5%) [21] and diluted accordingly to concentrations 0.1–100 μM (by distilled water). Then 20 μL of the solutions were added to each well and plates were incubated for 48 h. Also, 20 μL (5 mg/mL) of MTT (3-(4,5-dimethylthiazol-2-yl)-2,5-diphenyl-2H-tetrazolium bromide) reagent was added to each well. The cells were incubated at 37 °C in a CO_2 incubator for three or four hours. After the incubation period, the medium was removed and 200 μL DMSO added into each well to dissolve the produced formazan crystals by several pipetting up and down. The absorbance values at 540 nm were determined using an ELISA reader (Bio-Rad, Model 680, USA) [33]. The viability percent was obtained by dividing absorbance of the treated group to the absorbance of the control group, multiplied by 100 and results are expressed as IC_{50} (the concentration required to kill 50% of cells). Oxaliplatin was chosen as a positive reference. Untreated cells were run in each assay as the negative control group. All the experiments were performed in triplicate and data is registered as mean \pm S.E.M [27].

2.6. Statistical analysis

One-way analysis of variance (ANOVA) followed by Tukey's test (GraphPad version 5.0; GraphPad Software Inc, San Diego, CA) was used to obtain the difference between means. The value about $P < 0.05$ was considered to be statistically significant. Data are presented as mean \pm standard error in the results section.

Table 2
Selected bond lengths (Å) and angles (°) for (**L1**).

Bond lengths			
N(3)–C(14) ^{#1}	1.350(4)	N(1)–C(8)	1.347(4)
O(2)–C(1) ^{#2}	1.224(3)	N(1)–C(7)	1.403(4)
O(1)–C(1) ^{#2}	1.302(4)	C(3)–C(4)	1.380(4)
N(3)–C(15)	1.416(3)	O(4)–C(14)	1.212(3)
Bond angles			
O(4)–C(14)–N(3) ^{#1}	125.8(3)	N(2) ^{#1} –C(9)–C(8)	118.2(3)
O(5) ^{#3} –C(21)–O(6) ^{#3}	120.9(3)	N(2) ^{#1} –C(9)–C(10) ^{#4}	123.1(3)
O(2) ^{#2} –C(1)–O(1) ^{#2}	122.4(3)	O(5) ^{#3} –C(21)–C(20)	124.8(3)
O(2) ^{#2} –C(1)–C(2)	123.7(3)	O(3)–C(8)–N(1)	124.5(3)

Symmetry codes: #1: $-x + 1/2, y + 1/2, z$; #2: $-x + 1, -y, -z + 1$; #3: $-x + 1, -y + 1, -z + 1$; #4: $-x + 1/2, y - 1/2, z$.

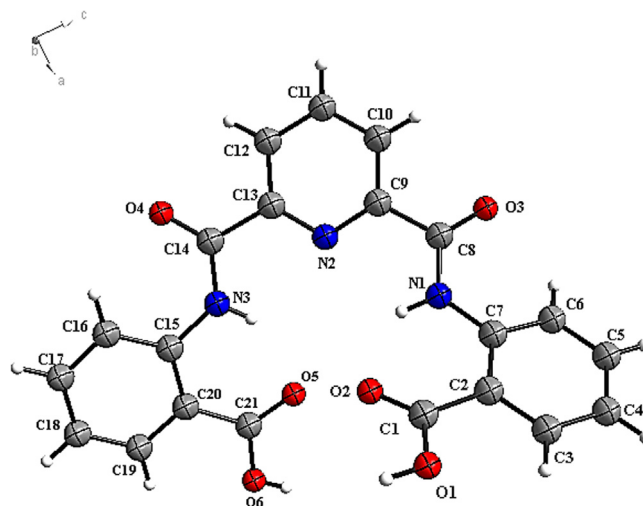


Fig. 1. Ball and stick diagram of the X-ray crystal structure of *N,N'*-bis(2-carboxylphenyl)-2,6-pyridinedicarboxamide, (**L1**), showing atomic numbering scheme with 50% probability.

3. Results and discussion

3.1. X-ray diffraction studies

3.1.1. Crystal structure of compound (**L1**)

To determine the geometry of compounds, single crystal X-ray analyses was performed for them. The procedure adopted in the synthesis of compounds is outlined in scheme 1.

Ligand (**L1**) has been crystallized in orthorhombic *Pbca* space group with eight molecules in the unit cell. A summary of crystallographic data is indicated in Table 1. Selected bond lengths and angles are presented in Table 2. The X-ray crystal structure of (**L1**) with atomic numbering scheme is represented in Fig. 1. On



Fig. 2. Hydrogen bonds existing between layers in the unit cell and formation of hydrogen bonding rings as $R_2^2(8)$ between carboxylic acid functional groups moieties (O–H...O), for *N,N'*-bis(2-carboxylphenyl)-2,6-pyridinedicarboxamide, (**L1**).

the base of crystallographic data, bis-amide structure of the compound (**L1**) reveals cis and trans geometries for the pyridine nitrogen to both NH and carbonyl groups, respectively. These groups are anticlinal and dihedral angles of the O(3)–C(8)–C(9)–N(2) and O(4)–C(14)–C(13)–N(2) were observed 167.50 and 174.93° respectively, for them [34]. Also, the angles between the central pyridine ring with two 2-carboxylphenyl rings are 34.88 and 21.93°. The obtained angles between the aromatic rings indicate that the ligand (**L1**) is not planar. The non-covalent interactions of hydrogen bonding in the crystal packing of the compound (**L1**) link the fragments of the layer like structure. These bonds with D...A distances ranging from 2.214(3) to 3.625(3) Å are exhibited in the crystal packing. Hydrogen bonding interactions have important role in the creation of the supramolecular network in (**L1**). In this structure, carboxylic acid functional groups moieties are held by hydrogen bonds. These interactions lead to formation of hydrogen bonding rings (synthons) as $R_2^2(8)$ (*R* for ring, 8 the number of atoms in the pattern, superscript 2 is the number of acceptor atoms and subscript 2 is the number of donor atoms) [27]. Hydrogen bonds existing between layers in the unit cell and the cyclic interactions are presented in Fig. 2. The organized hydrogen bonding interactions between O(1)–H(1)···O(2) [symmetry code: $-x+1, -y, -z+1$], O(6)–H(6)···O(2) and O(6)–H(6)···O(5) [symmetry code: $-x+1, -y+1, -z+1$] and C(18)–H(18)···O(3) [symmetry code: $x, -y+1/2, z-1/2$] contribute to the supramolecular arrangement (Fig. 2). The bonds of O(1)–H(1)···O(2) and O(6)–H(6)···O(5) are the strongest hydrogen bonds.

3.1.2. Crystal structure of compound (**L2**)

The crystallographic data indicated that the conversion of carboxylic acid groups to ester was done in accordance with prediction for ligand (**L2**). This Ligand was crystallized in monoclinic $P2_1/n$ space group with four molecules in the unit cell. The summary pertinent structural data is displayed in Table 1. The X-ray crystal structure with atomic numbering scheme is represented in Fig. 3. Selected bond distances and angles are shown in Table 3.

The configuration of the compound indicated rotation and orientation toward the outside of the molecule in one of 2-carboxyphenyl ethyl ester groups. It may be caused by the larger angle (54.71°) between two 2-carboxyphenyl rings than two 2-carboxyphenyl ethyl ester rings (43.94°). Like (**L1**), cis and trans geometries are observed for the pyridine nitrogen with both NH

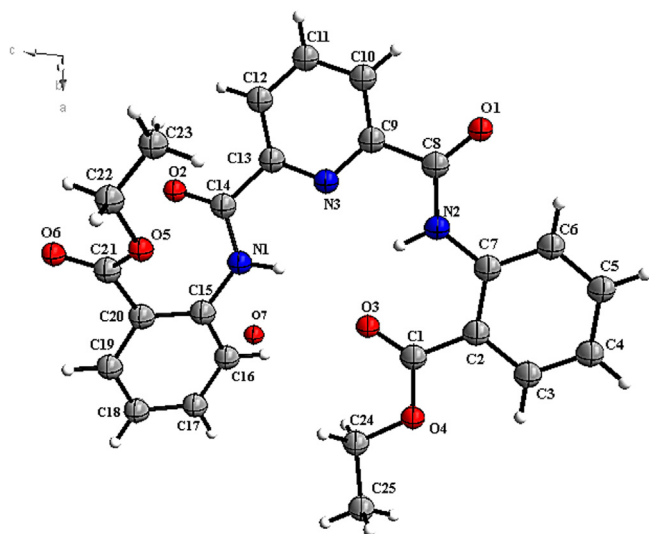


Fig. 3. Ball and stick diagram of the X-ray crystal structure of N,N'-bis(2-carboxyphenyl ethyl ester)-2,6-pyridinedicarboxamide, (**L2**), showing atomic numbering scheme with 50% probability.

Table 3
Selected bond lengths (Å) and angles (°) for (**L2**).

Bond lengths			
N(2)–C(8)	1.354(3)	N(3)–C(13)	1.337(3)
N(2)–C(7) ^{#1}	1.398(3)	N(1)–C(15)	1.420(3)
O(5)–C(21)	1.331(3)	C(7)–C(2) ^{#2}	1.414(4)
N(3)–C(9)	1.347(3)	O(1)–C(8)	1.219(3)
Bond angles			
O(2)–C(14)–N(1)	124.9(2)	N(2)–C(8)–C(9)	113.2(2)
O(6)–C(21)–O(5)	123.7(3)	N(2) ^{#1} –C(7)–C(6)	122.0(3)
O(3)–C(1)–O(4)	121.8(2)	C(18) ^{#2} –C(19)–C(20) ^{#2}	122.2(3)
O(1)–C(8)–C(9)	120.5(3)	O(4)–C(1)–N(2) ^{#1}	112.9(2)

Symmetry codes: #1: $-x+1, -y+1, -z+1$; #2: $-x+1/2+1, y+1/2, -z+1/2+1$.

and carbonyl groups, respectively. Also, these groups are anticlinal and dihedral angles of O(1)–C(8)–C(9)–N(3) and O(2)–C(14)–C(13)–N(3) groups are 174.83 and 177.51°, respectively. On the other hand, the angles 2.68 and 41.56° between the central pyridine ring with two 2-carboxyphenyl ethyl ester rings showed that compound (**L2**) is not planar [35].

The interactions of hydrogen bonding with D...A distances ranging from 2.634(4) to 3.869(5) Å are observed in the crystal packing of (**L2**). These interactions between amide moieties and pyridine fragments (C–H···O) led to the formation of hydrogen bond rings as $R_2^2(10)$. The cyclic interactions are displayed in Fig. 4. The hydrogen bonding interactions characteristic to the supramolecular arrangement are including C(10)–H(10)···O(1) [symmetry code: x, y, z] and C(4)–H(4)···O(5) [symmetry code: $-x+1, -y+2, -z+1$], in this structure. Also, co-crystallized one water molecule was observed along with ligand (**L2**), as disorder.

3.1.3. Crystal structure of compound (**3**)

Compound of $\{[Cu(CPCP)](DMAP) \cdot 3H_2O\}_n$ was crystallized from hot water as needle-like green single crystals in space group of monoclinic $P2_1/n$ with four molecules in the unit cell. A summary of crystallographic data is listed in Table 1. A schematic drawing

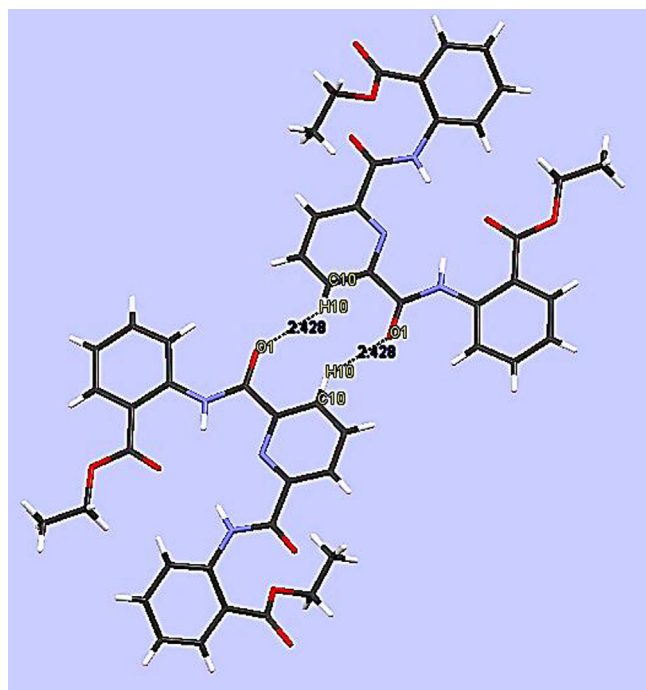


Fig. 4. Formation of hydrogen bonding rings as $R_2^2(10)$ between amide moieties and pyridine fragments (C–H···O), for N,N'-bis(2-carboxyphenyl ethyl ester)-2,6-pyridinedicarboxamide, (**L2**).

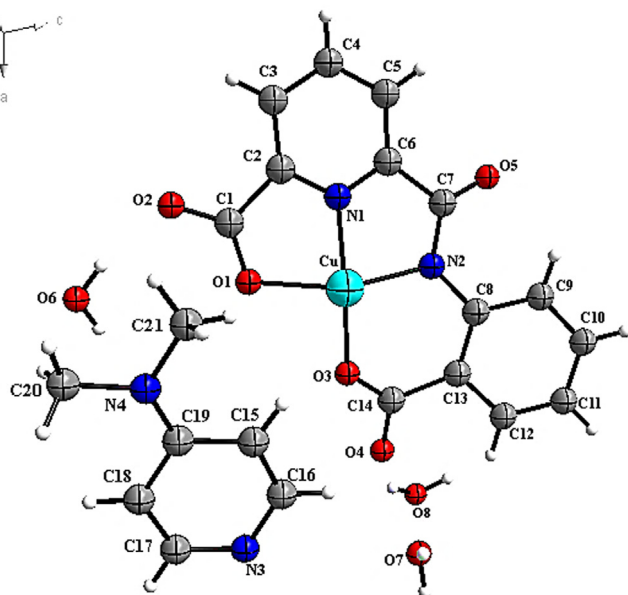


Fig. 5. Molecular structure of $[[\text{Cu}(\text{CPCP})](\text{DMAP})\cdot 3\text{H}_2\text{O}]_n$ (3), showing the atom numbering scheme with 50% probability of thermal ellipsoids.

of the complex and labeling of atoms is illustrated in Fig. 5. The packing pattern is displayed in Fig. 6a. The obtained data of X-ray investigations reveals that the formed complex is a one-dimensional polymer built up from asymmetric monomeric units in which the Cu(II) ion is surrounded by five donor atoms. The chelation in each of monomeric units is through two nitrogen (N1, N2) and two oxygen atoms (O1, O3) of the same monomer and one oxygen atom (O5) on an adjacent monomer. The zigzag bridging bonds of $[\text{Cu}-\text{O}(5) = 2.493(6) \text{ \AA} \{-x + 1/2, y - 1/2, -z + 1/2 + 1\}]$

between monomers cause that geometry around each copper ion to exhibit as a square pyramidal. In the overall structure of the complex, connectivity and extending is along [010] direction and polymeric chains are running parallel to the b axis. The intersected mean planes of the N(1)-pyridine and the N(2)-phenylcarboxylate rings were observed at $18.21(4)^\circ$ and the torsion angles values indicated at $\text{N}(2)-\text{Cu}-\text{O}(3)-\text{C}(14) = 1.66(6)$, $\text{N}(1)-\text{Cu}-\text{O}(1)-\text{C}(1) = -172.71(5)$, $\text{Cu}-\text{O}(3)-\text{C}(14)-\text{O}(4) = -170.11(5)$ and $\text{Cu}-\text{O}(1)-\text{C}(1)-\text{C}(1) = 6.23(8)^\circ$. Also Cu–Cu angle between the layers was observed at $81.24(3)^\circ$.

The bond lengths $\text{Cu}-\text{N}(1) = 1.887(5)$, $\text{Cu}-\text{O}(3) = 1.889(5)$, $\text{Cu}-\text{N}(2) = 1.982(5)$, $\text{Cu}-\text{O}(1) = 2.039(4) \text{ \AA}$ and the angles $\text{N}(1)-\text{Cu}-\text{O}(3) = 166.70(3)$, $\text{N}(1)-\text{Cu}-\text{N}(2) = 82.30(2)$, $\text{O}(3)-\text{Cu}-\text{N}(2) = 96.20(2)$, $\text{N}(1)-\text{Cu}-\text{O}(1) = 80.70(2)$, $\text{O}(3)-\text{Cu}-\text{O}(1) = 99.46(2)$, $\text{N}(2)-\text{Cu}-\text{O}(1) = 162.50(2)^\circ$ are comparable to other five-coordinated square pyramidal copper(II) complexes [1,36]. Selected bond lengths and angles are given in Table 4. In the crystal structure, in addition of the complex, co-crystallized one DMAP molecule and three water molecules are observed. Hydrogen bonding interactions between the complex with co-crystallized molecules of DMAP and water ($\text{O}-\text{H}\cdots\text{O}$ and $\text{O}-\text{H}\cdots\text{N}$ hydrogen bonds, range from 1.94 to 2.97 Å) led to the formation of the hydrogen bonding rings as $R_2^2(9)$, $R_3^3(9)$, $R_4^4(10)$. These interactions are shown in Fig. 6b. Strongest hydrogen bonds are including $[\text{O}(6)-\text{H}(6A)\cdots\text{O}(2)](x, y, z)$ and $[\text{O}(6)-\text{H}(6B)\cdots\text{N}(3)]\{-x + 1, -y, -z + 1\}$. Also, $\text{C}-\text{H}\cdots\pi$ stacking is observed between $\text{C}(20)-\text{H}(20C)$ and $(\text{N}3, \text{C}15-\text{C}19)$ of DMAP rings with distance of 3.686 Å and angle of 119.11° (Fig. 7).

3.2. Spectroscopic studies

The IR spectra of the ligands (L1) and (L2) exhibited that the stretching vibrations of amide carbonyl groups were appeared as strong absorption band at 1660 cm^{-1} for both the ligands [1]. While, the carbonyl groups stretching vibrations of

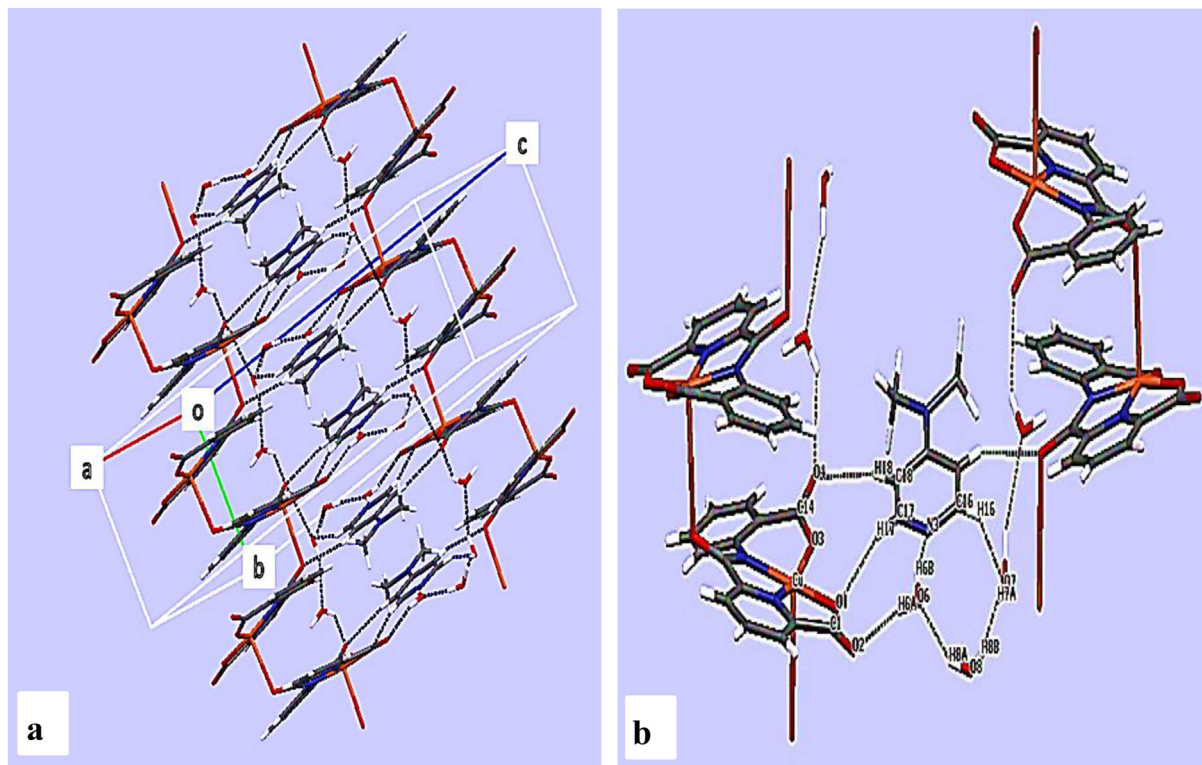
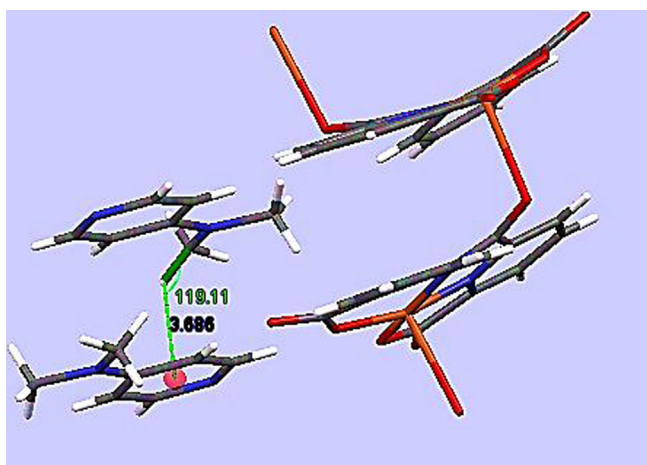


Fig. 6. a) Hydrogen bonds existing between layers in the unit cell; b) Formation of hydrogen bonding rings as $R_2^2(9)$, $R_3^3(9)$, $R_4^4(10)$ between complex, co-crystallized one DMAP molecule and three water molecules ($\text{O}-\text{H}\cdots\text{O}$ and $\text{O}-\text{H}\cdots\text{N}$), for complex (3).

Table 4
Selected bond lengths (Å) and angle (°) for (3).

Bond lengths					
Cu–N(1)	1.887(5)	C(14)–O(4)	1.253(8)	N(3)–C(17) ^{#2}	1.366(11)
Cu–N(2) ^{#1}	1.982(5)	N(1)–C(6)	1.322(8)	C(5)–H(5)	0.9300
Cu–O(1)	2.039(4)	N(1)–C(2)	1.344(8)	C(20)–H(20C)	0.9600
Cu–O(3)	1.889(5)	N(2)–C(7) ^{#1}	1.356(8)	C(2)–C(3)	1.379(8)
Cu–O(5) ^{#1}	2.493(6)	N(3)–C(8)	1.402(8)	C(5)–C(6)	1.390(9)
O(3)–C(14)	1.255(8)	N(4)–C(19)	1.315(10)	C(10)–C(11) ^{#3}	1.366(10)
O(2)–C(1)	1.244(8)	N(4)–C(21)	1.470(10)	O(7)–H(7A)	0.8501
O(1)–C(1)	1.272(8)	N(4)–C(20)	1.475(10)	O(8)–H(8B)	0.8499
Bond angles					
N(1)–Cu(1)–N(2) ^{#1}	82.30(2)	C(7) ^{#1} –N(2)–Cu(2) ^{#1}	114.2(4)	N(4)–C(21)–H(21B)	109.50
N(1)–Cu(1)–O(1)	80.70(2)	C(6)–N(1)–Cu(1)	118.4(4)	N(1)–C(6)–C(7) ^{#1}	112.80(6)
N(2) ^{#1} –Cu(1)–O(1)	162.50(2)	C(2)–N(1)–Cu(1)	119.10(4)	N(1)–C(6)–C(5)	120.30(6)
N(1)–Cu(1)–O(3)	166.70(3)	C(7) ^{#1} –N(2)–C(8)	123.50(6)	N(4)–C(19)–C(18) ^{#4}	121.40(7)
N(2) ^{#1} –Cu(1)–O(3)	96.20(2)	C(8)–N(2)–Cu(1) ^{#1}	122.30(4)	N(3)–C(15)–C(16)	123.20(8)
O(1)–Cu(1)–O(3)	99.46(19)	C(7) ^{#1} –N(2)–C(8)	123.50(6)	C(16)–N(3)–C(17) ^{#2}	116.60(8)
C(14) ^{#2} –O(3)–Cu(1)	128.00(5)	N(3) ^{#2} –C(17)–H(17)	117.70	C(17) ^{#4} –C(18)–H(18)	120.70
C(1)–O(1)–Cu(1)	128.00(5)	N(4)–C(21)–H(21A)	109.50	C(1)–C(2)–C(3)	128.70(6)

Symmetry codes #1: $-x + 1/2, y - 1/2, -z + 1/2 + 1$; #2: $-x + 1, -y, -z + 1$; #3: $-x + 1, -y, -z + 2$; #4: $-x + 1, -y - 1, -z + 1$.**Fig. 7.** C–H... π stacking between C(20)–H(20C) and (N3, C15–C19) of DMAP rings for complex (3).

2-carboxylphenyl and 2-carboxyphenyl ethyl ester rings were indicated as a weak band close to amide carbonyl group at 1693 and 1733 cm^{-1} for (L1) and (L2), respectively. The broad absorption bands in range 3229–3446 and 3138–3351 cm^{-1} manifested the presence of characteristic vibrations of –NH groups, for the compounds (L1) and (L2) [35,37]. The overlapping with OH broad band at this region causes that band of –NH seems as a weak doublet for (L1). Also a similar overlapping is observed for (L2) because of the presence of hydrogen bonds and water molecules [27]. Meaningful information can be obtained by comparing the IR spectra of the complex (3) and the uncomplexed ligand (L1). Coordination of the deprotonated carboxamide nitrogen and carboxylphenyl oxygen to the Cu(II) center resulted a shift to lower frequencies in the carbonyl vibrations. The carbonyl groups stretching vibrations of amide and acid were appeared at 1604 and 1647 cm^{-1} respectively, for (3). These vibrations shifted downward (about 46–56 cm^{-1}) compared to (L1), in agreement with the data reported for related complexes [38,39]. The appeared band at 3200–3446 cm^{-1} was assigned to the presence of hydrogen bonds and water molecules in the structure of complex [40]. The Cu–N and Cu–O stretching vibrations are found at around 510–542 and 685–752 cm^{-1} respectively, for complex (3) [41]. The compounds (L1) and (L2) displayed characteristic UV–Vis spectra at concentra-

tion 3×10^{-5} M in methanol, with an absorption maxima near 235 and 227 nm, assigned to $\pi \rightarrow \pi^*$ transition of the aromatic ring and shoulder at 327 and 311 nm corresponding to $n \rightarrow \pi^*$ transition of the C=O chromophore for (L1) and (L2), respectively [42,43]. For studies of metal complexation, electronic absorption spectrum of the compound (3) was performed at concentration 3×10^{-3} M in methanol and it indicated only one broad $d-d$ transition band at ≈ 656 nm ($\epsilon = 69 \text{ mol}^{-1} \text{ L cm}^{-1}$), corresponding to the ${}^2E_g \rightarrow {}^2T_{2g}$ transition [41], that suggests octahedral configuration for the copper ion. The change in configuration around the copper ion in solution with obtained square pyramidal geometry of X-ray in solid state, can be justified by the coordination of one molecule of solvent in axial position of copper ions [27]. The other expected band at 345–391 nm is attributed to the charge transfer transitions. Also, $\pi \rightarrow \pi^*$ and $n \rightarrow \pi^*$ intra-ligand charge transitions at 231 and 272 nm were observed for the complex (3), which exhibited hypsochromic shift about 55 nm in absorption band of $n \rightarrow \pi^*$ of the complex (3) than the ligand (L1). The observed shift could be due to the donation of a lone pair of carbonyl electrons of pyridine-2,6-dicarbonyl to copper(II) ion [26], corresponding to the obtained structure of X-ray crystallography. The electronic impact mass spectrum provides good evidence for the molecular formula of the synthetic compounds [44]. The mass spectra of the ligands (L1) and (L2) showed m/z peaks at 405 and 479 that corresponded to $\text{C}_{21}\text{H}_{15}\text{N}_3\text{O}_6$ and $\text{C}_{25}\text{H}_{25}\text{N}_3\text{O}_7$ moieties, respectively. The selected series of peaks with values, i.e. 375, 342, 314, 286 u corresponding to $[\text{C}_{20}\text{H}_{13}\text{N}_3\text{O}_5]$, $[\text{C}_{19}\text{H}_8\text{N}_3\text{O}_4]$, $[\text{C}_{19}\text{H}_8\text{NO}_4]$, $[\text{C}_{17}\text{H}_4\text{NO}_4]$ for (L1) and 441, 417, 375, 341 u corresponding to $[\text{C}_{25}\text{H}_{19}\text{N}_3\text{O}_5]$, $[\text{C}_{23}\text{H}_{19}\text{N}_3\text{O}_5]$, $[\text{C}_{20}\text{H}_{13}\text{N}_3\text{O}_5]$, $[\text{C}_{20}\text{H}_9\text{N}_2\text{O}_4]$ for (L2) are attributable to different fragments of the ligands. Similarly, mass spectrum of the complex (3) exhibited molecular ion peak [M] at m/z 522, which agree well with the molecular formula that is $\{[\text{Cu}(\text{CPCP})](\text{DMAP})\cdot 3\text{H}_2\text{O}\}_n$ and suggests the monomeric nature for the complex (3) [45]. Also, fragments peaks at m/z 377, 341, 313, 264, 236 and 200 are corresponding to $[\text{C}_{14}\text{H}_{10}\text{N}_4\text{O}_5\text{Cu}]$, $[\text{C}_{14}\text{H}_6\text{N}_4\text{O}_3\text{Cu}]$, $[\text{C}_{14}\text{H}_6\text{N}_2\text{O}_3\text{Cu}]$, $[\text{C}_{14}\text{H}_5\text{N}_2\text{Cu}]$, $[\text{C}_{13}\text{H}_3\text{NCu}]$ and $[\text{C}_{10}\text{H}_3\text{NCu}]$, respectively. The obtained results of both elemental analysis and mass spectra of the compounds are in good agreement with the proposed formula for them.

4. Thermal studies of complex

The TGA/DTA scanning were carried out within a temperature range from 30 to 800 $^\circ\text{C}$ in N_2 atmosphere at a rate of 10 $^\circ\text{C}/\text{min}$

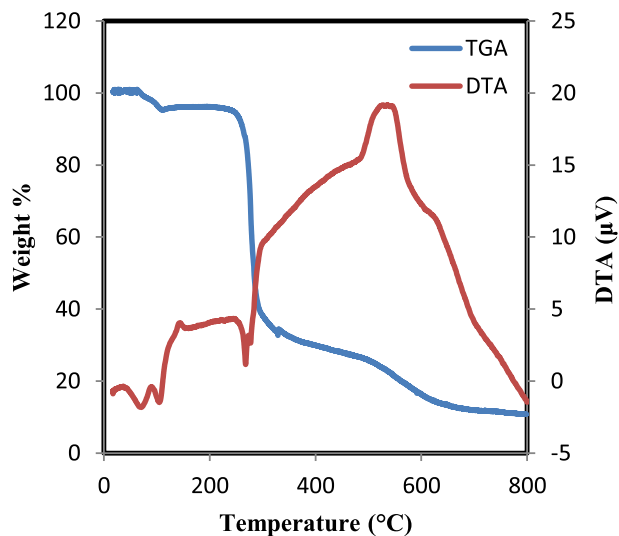


Fig. 8. Thermal behavior of complex (3).

to measure the percentage of mass loss as a function of temperature [46] on crystalline sample of the compound (3).

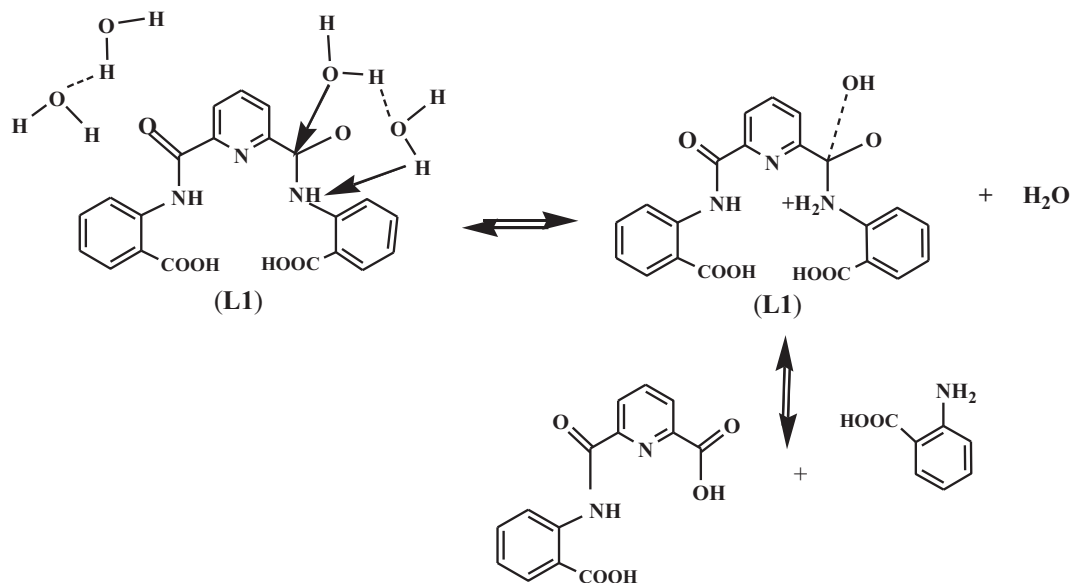
Thermogravimetric (TG) analysis exhibited three-step decomposition processes for the complex (3) in which weight loss starts at 60 and ends at 745 °C (Fig. 8). The first decomposition step at 60–100 °C with the loss weight of 6.01% is assignable to the removal of co-crystallized two water molecules (H_4O_2) in structure (calcd 6.89%). The second decomposition step occurs at 100–405 °C with total weight loss about of 65.90% due to the removal of co-crystallized one water molecule, one DMAP molecule and also pyridine 2-carboxylate-6-carboxamide molecule ($C_{14}H_{15}N_4O_4$) from crystalline sample (calcd 62.34%). The third decomposition step at 410–745 °C with mass loss of 17.92% can be attributed to the elimination of two oxygen atoms (O_2) in carboxylate phenyl (calcd 17.48%). The residual structure is expected to be copper uncoordinated to phenyl ring as final product. The obtained curve of differential thermal analysis (DTA) indicates three distinct endothermic peaks at 52, 84 and 264 °C and three distinct exothermic peaks at 81, 135 and 518 °C. The collected data of TGA-DTA curves of (3)

during decomposition steps is in an excellent agreement with together and also with the obtained structure of the crystallographic studies.

5. Esterification and hydrolysis mechanisms of (L1)

The ligand (L1) was synthesized as compound with functional groups of amide and carboxylic acid corresponding to prediction and (L2) was prepared on the base of conversion of carboxylic acid groups to ester in (L1), using acid (As catalyst) and alcohol (Fischer esterification). Ethanol is used as solvent. So, it is in excess. Different acids can be used for this conversion, but H_2SO_4 (Sulfuric acid) and TsOH (Tosic acid) are often used. In replacement of OH by OR, many steps were exhibited including: protonation of the carbonyl oxygen by acid for making the carbonyl carbon to much better electrophile, 1,2-addition by the alcohol for transfer of the proton from the alcohol to one of the OH groups, 1,2-elimination of water, protonation of ester and then deprotonation of it. All these steps are in equilibrium and byproduct of the reaction is water.

Study of crystal structure of (3) confirmed that the ligand (L1) was hydrolyzed during the reaction with the metal salt and one of the *N*-carboxylphenyl bonds is broken in it. With regard to high stability of amide bonds towards hydrolysis [47], no more studies have been reported about the hydrolysis of amide ligands during complexation. It seems that, the factors such as Cu(II) catalytic effects, electrophilic (carbonyl) activation and intermolecular metal hydroxide mechanisms [48], ligand architecture and its coordination modes [49], the concentration of effective anions, hydrogen ions and temperature [16] can be effective in the hydrolysis rate. Generally, amides can be hydrolyzed depending on the pH under either acidic or basic conditions and or from water-assisted pathway [50,51], but the mechanism of the catalyzed hydrolysis reaction is not still obvious [52]. With assuming the water-assisted route, possible mechanism is shown in Scheme 2. In this case, steric effects may be a barrier of same orientation and interaction of the water molecules toward both amide groups and as a result, one of the amide groups is not hydrolyzed. But determination of the accurate route and effective factors on hydrolysis of the ligand (L1) during formation of the complex is difficult in this work and more accurate studies must be supported by experimental works which is not within our goals.



Scheme 2. Hydrolysis of water-assisted pathway in (L1).

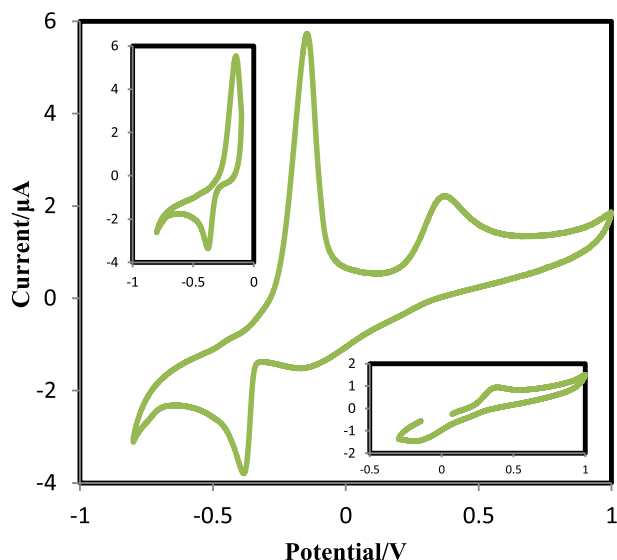


Fig. 9. Cyclic voltammogram of complex (3), $c = 4 \times 10^{-3} \text{ mol/dm}^3$ in H_2O medium, KCl (0.1 M) at GCE, scan rate 0.05 V/s.

6. Electrochemical properties

The electrochemical behavior of the compounds (**L1**), (**L2**) and (**3**) were studied using cyclic voltammetry with potential in the range -1.0 to $+1.0$ V and scan rate of 0.05 V s^{-1} , in methanol solution containing 0.1 M LiClO_4 as supporting electrolyte for the compounds (**L1**), (**L2**) and in aqueous solution containing 0.1 M KCl as supporting electrolyte for the complex (**3**). No redox response was observed in the ligands (**L1**) and (**L2**). The cyclic voltammogram for the compound (**3**) is displayed in Fig. 9.

As seen, two anodic peaks appeared from -0.32 to $+0.57$ V at $E_{A1} = -0.16$ and $E_{A2} = 0.32$ V and in the reverse cycle, two cathodic peaks are observed from 0.05 to -0.53 at $E_{C2} = -0.16$ (as a wide wave with potential approx equal to anodic peak) and $E_{C1} = -0.36$ V. The first quasi reversible couple with $E^{0'} = -0.26$ V, $E_{C1} = -0.36$ V and $E_{A1} = -0.16$ V was assigned to Cu(I)/Cu(0) redox system. The anodic peak height is attributed to the Cu(0) deposit oxidation to Cu(I). The high value of the first anodic peak current can be explained by the redissolution of copper electrodeposited during the forward potential scan [53]. The peak separation (ΔE_p) is 0.20 V, for this couple.

The second couple with $E^{0'} = 0.08$ V, $E_{C2} = -0.16$ V and $E_{A2} = 0.32$ V was corresponding to Cu(II)/Cu(I) redox process. The peak separation (ΔE_p) was 0.48 V, for this couple. Redox process of Cu(I)/Cu(0) occurred at more negative $E^{0'}$ potential compared to Cu(II)/Cu(I) [54]. The obtained results of the investigation of the cyclic voltammogram of the ligand (**L1**) confirm that it did not exhibit any wave in the potential range of -1.0 to $+1.0$ V, thus the observed redox couples have been assigned to single electron transfer processes in the metal center of the complex [55].

7. Catalytic activity

Selective oxidation of alcohols into the corresponding carbonyl compounds has occupied an outstanding part of the modern synthetic organic chemistry [56,57]. Because of the importance of aldehydes in the production of fine chemicals such as food additives or fragrances [58,59], conversion of primary alcohols to aldehydes has been attracting researchers' attention. The catalytic activity of the complex (**3**) with change in the amount of it has been summarized in Table 5. As shown, the complex is active enough on the oxidation of benzyl alcohol. It indicates that the complex as catalyst is necessary to run the oxidation reaction. The effect of hydrogen peroxide as oxidant on the oxidation of benzyl alcohol is displayed in Table 6. The results show that the reaction yield increased by increasing the amount of hydrogen peroxide. The maximum yield is obtained of 81% by applying 0.04 g of the complex and $60 \mu\text{L}$ of hydrogen peroxide. The effect of temperature on the reaction yield is indicated in Table 7. The investigations showed that the optimum temperature is 45°C for the reaction. It is seen that the reaction yield does not change by rising the temperature. After realization of the optimized conditions (amount of catalyst 0.04 g , reaction temperature 45°C , used amount H_2O_2 $60 \mu\text{L}$), oxidation of a number of benzyl alcohol derivatives and hexanol was studied in the presence of the complex as catalyst. The obtained selectivity and yield of the compounds are indicated in Table 8. In this study the complex showed outstanding catalytic performance with selective conversion of alcohols at 45°C . This high activity and selectivity is likely related to lewis acidity of the catalyst [60]. In conclusion, oxidation of benzyl alcohol using hydrogen peroxide as mild oxidant in the presence of synthetic complex as catalyst provides an efficient, easy and safe approach for oxidation of alcohols to the corresponding aldehydes.

8. Stability testing of complex (3)

The stability of the complex (**3**) was evaluated by UV–Vis spectral analysis at different times in a mixture containing DMSO/ H_2O at concentration of $100 \mu\text{M}$, 37°C and pH 7.2. The degree of decomposition over time was determined by comparing the spectra collected after 0, 1, 24, and 48 h. The results indicated that the values of absorbance and wavelength were not affected, even after 48 h and confirmed that the complex is stable in the solution for at least 48 h under the test conditions [27].

9. Cytotoxicity

The *in vitro* anticancer activity of the synthetic compounds was studied on MCF7, HT29 and βTC cell lines by the MTT method and using oxaliplatin as a positive control. The obtained results after 48 h of the treatment on the cell lines are displayed in Fig. 10 and Table 9. The cell proliferation was exhibited for all the three compounds in the dose-dependent manner. The ligands (**L1**) and (**L2**) indicated close anti-proliferative effect to oxaliplatin on

Table 5
Catalytic effect of complex (**3**) on the oxidation of benzyl alcohol with different amounts of catalyst.

Entry	Oxidant (30 μL)	Complex (g)	Product	Selectivity (%)	Yield (%)
1	H_2O_2	0.01	Benzaldehyde	>99	21
2	H_2O_2	0.02	Benzaldehyde	>99	22
3	H_2O_2	0.03	Benzaldehyde	>99	28
4	H_2O_2	0.04	Benzaldehyde	>99	41
5	H_2O_2	0.045	Benzaldehyde	>99	41
6	H_2O_2	0.05	Benzaldehyde	>99	40
7	H_2O_2	Not used	Benzaldehyde	>99	3

Table 6

Effect of hydrogen peroxide on the oxidation of benzyl alcohol in the presence of optimized amount of catalyst.

Entry	H ₂ O ₂ (μl)	Complex (g)	Product	Selectivity (%)	Yield(%)
1	30	0.04	Benzaldehyde	>99	41
2	35	0.04	Benzaldehyde	>99	53
3	40	0.04	Benzaldehyde	>99	62
4	45	0.04	Benzaldehyde	>99	69
5	55	0.04	Benzaldehyde	>99	78
6	60	0.04	Benzaldehyde	> 99	81
7	65	0.04	Benzaldehyde	> 99	80

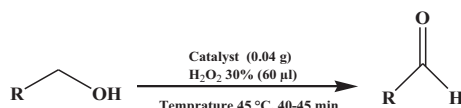
Table 7

Effect of temperature on the oxidation of benzyl alcohol in the presence of optimized amounts of catalyst and hydrogen peroxide.

Entry	H ₂ O ₂ (μl)	Complex (g)	Temperature(°C)	Product	Yield(%)
1	60	0.04	20	Benzaldehyde	47
2	60	0.04	37	Benzaldehyde	64
3	60	0.04	40	Benzaldehyde	86
4	60	0.04	45	Benzaldehyde	93
5	60	0.04	55	Benzaldehyde	92
6	60	0.04	65	Benzaldehyde	90
7	60	0.04	70	Benzaldehyde	84

Table 8

Oxidation of benzyl alcohol derivatives and hexanol in the presence of complex (3) as catalyst under the optimized conditions.



Entry	Substrate	Product	Selectivity (%)	Isolated Yield (%)
1			>99	92
2			>99	93
3			>99	93
4			>99	87
5			>99	86
7			>99	72

Amount of catalyst 0.04 g, amount of H₂O₂ 60 μL, reaction temperature 45 °C, 0.5 mmol substrate.

MCF7 and βTC cell lines at the concentrations 0.1–100 μM, while HT29 cells exhibited the higher sensitivity to the ligand (**L1**) (with IC₅₀ equal to 10 μM) compared to oxaliplatin at concentrations 10–100 μM. On the other hand, no significant difference was displayed between (**L2**) and oxaliplatin on HT29 cells at all the tested concentrations (both with IC₅₀ values about 100 μM). The complex (**3**) exhibited a significant cytotoxic effect (with IC₅₀ = 1 μM) compared to oxaliplatin and both of the ligands on MCF7 and HT29 cells, also it had a moderate *anti*-proliferative effect (with IC₅₀ = 10 μM), than oxaliplatin on βTC cell line. This rate of inhibitory is considerable with regarding to lack of response to

therapeutic agents in treatment of pancreatic cancer [61,62]. In general, the complex (**3**) showed the highest cytotoxicity effect compared to the ligands (**L1**) and (**L2**) on all the three cell lines. Accordingly, it is reasonable to assume that inhibitory effect of organic compounds can be increased by chelation with metal ions. These results are comparable to those reported previously [63–65]. It should be noted that metal complexes as drug display enhanced selectivity and novel modes of DNA interaction, like non-covalent interactions that mimic the interaction mode of biomolecules [66]. However to evaluate metal complexes as therapeutic agents further studies are needed under biological conditions.

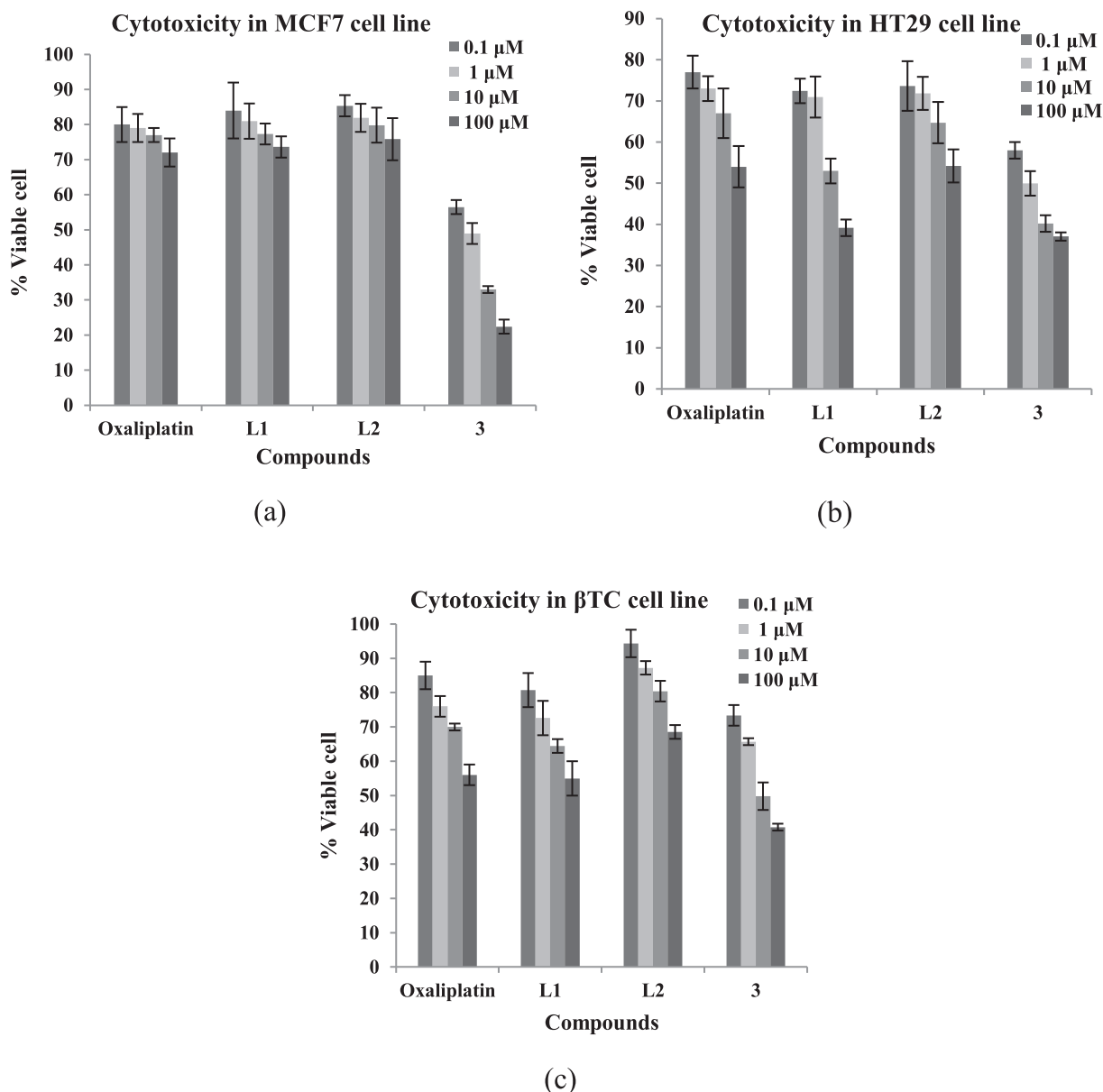


Fig. 10. Cytotoxic effect of oxaliplatin and synthetic compounds (**L1**), (**L2**) and (**3**) against a) MCF7, b) HT29 and c) βTC cell lines. The incubated cells were treated with concentrations 0.1, 1, 10 and 100 μM of compounds. Cytotoxicity was determined under MTT method as explained. Data are registered as mean ± S.E.M (n = 3).

Table 9

IC₅₀ determination of compounds (**L1**), (**L2**) and (**3**) against MCF7, HT29 and βTC cell lines.

IC ₅₀ (μM ± s.d.)			
Compounds	MCF7	HT29	βTC
L1	>100 ± 4.2	10 ± 6.3	>100 ± 4.4
L2	>100 ± 6.3	100 ± 4.1	>100 ± 5.3
3	1 ± 3.1	1 ± 3.4	10 ± 4.2
Oxaliplatin	>100 ± 6.2	100 ± 5.1	>100 ± 5.6

%Viability ± standard error is expressed as an average of triplicates.

10. Conclusion

Two novel ligands (**L1**), (**L2**) and a polymeric copper (II) complex (**3**) from (**L1**) were synthesized. X-ray crystallographic studies of complex (**3**) revealed a square pyramidal geometry around copper ion along with co-crystallized molecules of DMAP and water.

The study of compounds electrochemical properties proved that only complex (**3**) is involved in redox reactions. According to the obtained results, it is inferred that complex (**3**) as catalyst is active enough on the oxidation of aromatic and aliphatic alcohols. Also, after MTT assay, it was manifested that complex (**3**) has stronger cytotoxicity than oxaliplatin and both ligands against all the three cell lines.

Acknowledgments

We would like to thank the University of Kurdistan and Faculty of Pharmacy of Tehran University of Medical Sciences for financial support.

Appendix A. Supplementary data

CCDC 1478768–1478770 contains the supplementary crystallographic data for compounds (**1**)–(**3**) respectively. These data can be

obtained free of charge via <http://www.ccdc.cam.ac.uk/conts/retrieving.html>, or from the Cambridge Crystallographic Data Centre, 12 Union Road, Cambridge CB2 1EZ, UK; fax: (+44) 1223-336-033; or e-mail: deposit@ccdc.cam.ac.uk.

Supplementary data associated with this article can be found in the online version, at <http://dx.doi.org/10.1016/j.ica.2017.02.023>.

References

- [1] A.K. Patra, M. Ray, R.M. Mukherjee, *J. Chem. Soc. Dalton Trans.* 15 (1999) 2461–2466.
- [2] A.G. Galinos, S.P. Perlepes, T.F. Zafropoulos, P.V. Ioannou, J.K. Kouinis, *Monatsh. Chem.* 112 (1981) 1113–1121.
- [3] M.A. Kadir, N. Mansor, M.S.M. Yusof, C.J. Sumbly, *Complex Met.* 1 (2014) 32–37.
- [4] T.C. Woon, D.P. Fairlie, *Inorg. Chem.* 31 (1992) 4069–4074.
- [5] M. Dasgupta, S. Nag, G. Das, M. Nethaji, S. Bhattacharya, *Polyhedron* 27 (2008) 139–150.
- [6] E.V. Savinkina, I.A. Zamilatskov, A.S. Kuzovlev, D.V. Albov, D.V. Golubev, V.V. Chernyshev, *Polyhedron* 69 (2014) 68–76.
- [7] O. Clement, B.M. Rapko, B.P. Hay, *Coord. Chem. Rev.* 170 (1998) 203–243.
- [8] G. Sanchez, J. Garcia, J.J. Ayllon, J.L. Serrano, L. Garcia, J. Perez, G. Lopez, *Polyhedron* 26 (2007) 2911–2918.
- [9] L. Zhao, H. Ding, B. Zhao, C. Lu, Y. Yao, *Polyhedron* 83 (2014) 50–59.
- [10] S. Meghdadi, V. Mirkhani, R. Kia, M. Moghadam, S. Tangestaninejad, I. Mohammad poor-Baltork, *Polyhedron* 41 (2012) 115–119.
- [11] E.E.S. Teotonio, H.F. Brito, G.F. de Sa, M.C.F. Felinto, R.H.A. Santos, R.M. Fuquen, I.F. Costa, A.R. Kennedy, D. Gilmore, W.M. Faustino, *Polyhedron* 38 (2012) 58–67.
- [12] H. Sigel, R.B. Martin, *Chem. Rev.* 82 (1982) 385–426.
- [13] Y. Tang, L.N. Zakharov, A.L. Rheingold, R.A. Kemp, *Polyhedron* 24 (2005) 1739–1748.
- [14] L.M.L. Miguel, S.O. Hisila, N.R. Elena, M.L. Lorena, S.M. Rocio, O.L. Karen, *Polyhedron* 79 (2014) 338–346.
- [15] R.Y. Wang, L. Wu, Y.H. Yu, X.X. Zhang, B.L. Wu, H.Y. Zhang, *Polyhedron* 45 (2012) 170–176.
- [16] M. Munjal, S. Kumar, S.K. Sharma, R. Gupta, *Inorg. Chim. Acta* 377 (2011) 144–154.
- [17] A.C. Valderrama-Negron, W.A. Alves, A.S. Cruz, S.O. Rogero, D.O. Silva, *Inorg. Chim. Acta* 367 (2011) 85–92.
- [18] M. Amini, A. Bayrami, M.N. Marashi, A. Arab, A. Ellern, L.K. Woo, *Inorg. Chim. Acta* 443 (2016) 22–27.
- [19] P.A.N. Reddy, R. Datta, A.R. Chakravarty, *Inorg. Chem. Commun.* 3 (2000) 322–324.
- [20] E. Haldon, M.D. Rebollo, A. Prieto, E. Alvarez, C. Maya, M.C. Nicasio, P.J. Perez, *Inorg. Chem.* 53 (2014) 4192–4201.
- [21] J.C. Almeida, D.A. Paixao, I.M. Marzano, J. Ellena, M. Pivatto, N.P. Lopes, A.M.D. C. Ferreira, E.C.P. Maia, S. Guilardi, W. Guerra, *Polyhedron* 89 (2015) 1–8.
- [22] A.Q. Ali, S.G. Teoh, N.E. Eltayeb, M.B.K. Ahamed, A.M.S. Abdul Majid, *Polyhedron* 74 (2014) 6–15.
- [23] M. Ganeshpandian, R. Loganathan, S. Ramakrishnan, A. Riyasdeen, M.A. Akbarsha, M. Palaniandavara, *Polyhedron* 52 (2013) 924–938.
- [24] P. Pattanayak, J.L. Pratihari, D. Patra, P. Brandao, V. Felix, S. Chattopadhyay, *Polyhedron* 79 (2014) 43–51.
- [25] A.E. Patterson, J.J. Miller, B.A. Miles, E.L. Stewart, J.M. Melanson, C.M. Vogels, A. M. Cockshutt, A. Decken, P. Morin, S.A. Westcott, *Inorg. Chim. Acta* 415 (2014) 88–94.
- [26] K.B. Gudasi, S.A. Patil, R.S. Vadavi, R.V. Shenoy, M.S. Patil, *J. Serb. Chem. Soc.* 71 (2006) 529–549.
- [27] S. Abdolmaleki, M. Ghadermazi, A. Fattahi, S. Sheshmani, *Inorg. Chim. Acta* 443 (2016) 284–298.
- [28] (a) Bruker AXS Inc., SMART (Version 5.060) and SAINT (Version 6.02), Madison, Wisconsin, USA, 1999;
- (b) M.C. Burla, R. Caliandro, M. Camalli, B. Carrozzini, G.L. Cascarano, L. De Caro, C. Giacovazzo, G. Polidori, R. Spagna, *J. Appl. Cryst.* 38 (2005) 381–388;
- (c) G.M. Sheldrick, SHELXL97. Program for Crystal Structure Refinement, University of Göttingen, Germany, 1997;
- (d) SHELXT LN, Version 5.10, Bruker Analytical X-ray Inc., Madison, WI, USA, 1998;
- (e) W. Shi, X.-Y. Chen, B. Zhao, A. Yu, H.-B. Song, P. Cheng, H.-G. Wang, D.-Z. Liao, S.-P. Yan, *Inorg. Chem.* 45 (2006) 3949–3957.
- [29] L.J. Farrugia, *J. Appl. Crystallogr.* 32 (1999) 837–838.
- [30] K. Brandenburg, M. Berndt, *J. Appl. Crystallogr.* 32 (1999) 1028–1029.
- [31] C.F. Macrae, P.R. Edgington, P. McCabe, E. Pidcock, G.P. Shields, R. Taylor, M. Towler, J. van de Streek, *J. Appl. Crystallogr.* 39 (2006) 453–457.
- [32] A.R. Judy Azar, E. Safaei, S. Mohebbi, *Mater. Res. Bull.* 70 (2015) 753–761.
- [33] A. Fattahi, M.A. Golozara, J. Varshosazb, H.M. Sadeghid, M. Fathi, *Carbohydr. Polym.* 87 (2012) 1176–1184.
- [34] P. Devi, S.M. Barry, K.M. Houlihan, M.J. Murphy, P. Turner, P. Jensen, P.J. Rutledge, *Sci. Rep.* 5 (2015) 1–6.
- [35] Y. Perez, A.L. Johnson, P.R. Raithby, *Polyhedron* 30 (2011) 284–292.
- [36] M. Mirzaei, V. Lippolis, M.C. Aragoni, M. Ghanbari, M. Shamsipur, F. Meyer, S. Demeshko, S.M. Pourmortazavi, *Inorg. Chim. Acta* 418 (2014) 126–135.
- [37] S.L. Jain, P. Bhattacharyya, H.L. Milton, A.M.Z. Slawin, J.A. Crayston, J.D. Woollins, *Dalton Trans.* 6 (2004) 862–871.
- [38] E. Wagner-Wysiecka, J. Chojnacki, *Supramol. Chem.* 24 (2012) 684–695.
- [39] L.S.V. Jesic, L.S. Jovanovic, V.M. Leovac, M.M. Radanovic, M.V. Rodic, B.B. Hollo, K.M. Szecsenyi, S.A. Ivkovic, *Polyhedron* 101 (2015) 196–205.
- [40] A.I. El-Said, A.A.M. Aly, M.S. El-Meligy, M.A. Ibrahim, *J. Argent. Chem. Soc.* 97 (2009) 149–165.
- [41] A.S. Kindeel, I.J. Dawood, M.R. Aziz, *J. Baghdad for Sci.* 1 (2013) 396–404.
- [42] A.A. El-Bindary, A.Z. El-Sonbati, *Polish J. Chem.* 74 (2000) 615–620.
- [43] A.M.K.R. Balan, R. Francis Nicholas Ashok, M. Vasanthi, R. Prabu, A. Paulraj, *Int. J. Life Sci Pharm. Res.* 3 (2013) 67–75.
- [44] W.H. Mahmoud, G.G. Mohamed, M.M.I. El-Dessouky, *J. Mol. Struct.* 1082 (2015) 12–22.
- [45] P. Rath, D.P. Singh, *J. Mol. Struct.* 1100 (2015) 208–214.
- [46] D.M. Fouad, A. Bayoumi, M.A. El-Gahami, S.A. Ibrahim, A.M. Hammam, *Nat. Sci.* 2 (2010) 817–827.
- [47] S. Mallakpour, H. Yousefian, *J. Braz. Chem. Soc.* 18 (2007) 1220–1223.
- [48] L.M. Sayre, K.V. Reddy, A.R. Jacobson, W. Tang, *Inorg. Chem.* 31 (1992) 935–937.
- [49] S. Kumar, R.R. Jha, S. Yadav, R. Gupta, *New J. Chem.* 39 (2015) 2042–2051.
- [50] D. Zahn, *J. Chem. Phys.* 300 (2004) 79–83.
- [51] D. Zahn, *Eur. J. Org. Chem.* 19 (2004) 4020–4023.
- [52] C.J. GifSney, C.J. O'Connov, *Aust. J. Chem.* 29 (1976) 307–314.
- [53] R. Drissi-Daoudi, A. Irhzo, A. Darchen, *J. Appl. Electrochem.* 33 (2003) 339–343.
- [54] V. Sargentelli, A.V. Benedetti, A.E. Mauro, *J. Braz. Chem. Soc.* 8 (1997) 271–274.
- [55] L. Fotouhi, S. Dehghanpour, M.M. Heravi, M. Dashti Ardakani, *Molecules* 12 (2007) 1410–1419.
- [56] M. Uyanik, K. Ishihara, *Chem. Commun.* 16 (2009) 2086–2099.
- [57] M. Uyanik, M. Akakura, K. Ishihara, *J. Am. Chem. Soc.* 131 (2009) 251–262.
- [58] R.A. Sheldon, I.W.C.E. Arends, A. Dijkstra, *Catal. Today* 57 (2000) 157–166.
- [59] M. Musawir, P.N. Davey, G. Kelly, I.V. Kozhenikov, *Chem. Commun.* 12 (2003) 1414–1415.
- [60] A.C. Raimondi, V.R. de Souza, H.E. Toma, D.J. Evans, T. Hasegawa, F.S. Nunes, *Spectrochim. Acta Mol. Biomol.* 61 (2005) 1929–1932.
- [61] M.W. Saif, *J. Pancreas* 9 (2008) 403–407.
- [62] P. Ghaneh, E. Costello, J.P. Neoptolemos, *Gut* 56 (2007) 1134–1152.
- [63] M. Grazul, A. Kufelnicki, M. Wozniczka, I.P. Lorenz, P. Mayer, A.J. Wiak, M. Czyz, E. Budzisz, *Polyhedron* 31 (2012) 150–158.
- [64] S.B. Kumar, Z. Mahendrasinh, S. Ankita, R. Mohammedayaz, P. Pragna, E. Suresh, *Polyhedron* 36 (2012) 15–20.
- [65] S. Mathan Kumar, K. Dhahagani, J. Rajesh, K. Anitha, G. Chakkaravarthi, N. Kanakachalam, M. Marappan, G. Rajagopal, *Polyhedron* 85 (2015) 830–840.
- [66] N. Nanjundan, R. Narayanasamy, S. Geib, K. Velmurugan, R. Nandhakumar, M. D. Balakumaran, P.T. Kalaichelvan, *Polyhedron* 110 (2016) 203–220.